Performance Evaluation of Cardiac Repolarization Markers Derived from Unipolar Electrograms and Monophasic Action Potentials: A Simulation Study

P Colli Franzone[1], LF Pavarino[2], S Scacchi[1], B Taccardi[3]

[1]Department of Mathematics, University of Pavia, Italy
[2]Department of Mathematics, University of Milan, Italy
[3]CVRTI, University of Utah, USA

Abstract

Objectives. The aim of this work is to provide a quantitative analysis of cardiac repolarization time (RT) markers derived from unipolar electrograms (EGs) and hybrid monophasic action potentials (HMAPs) under normal and ischemic conditions. These markers are compared with the gold standard RT markers based on the transmembrane action potential (TAP).

Methods. The analysis is based on large scale parallel 3D numerical simulations of the action potential propagation modeled by the anisotropic Bidomain system coupled with the Luo-Rudy I membrane model. Activation and recovery sequences elicited by local stimulus are simulated in an insulated block of cardiac tissue with rotational fiber anisotropy, homogeneous intrinsic cellular properties and in presence of an ischemic region.

Results. We found a very high correlation (> 0.98) between any of the EG- or HMAP-based markers and the associated TAP-based markers, for tissues with both homogeneous cellular properties and in presence of an ischemic region. Despite this good global match, our results also show that the EG-based markers may be locally inaccurate and fail to provide reliable estimates of the TAP-based markers in some critical conditions.

Conclusions. Highly reliable repolarization sequences can be derived from the extracellular RT markers. Moreover, the HMAP-based markers may offer a reliable alternative for estimating the TAP-based markers when the EG-based markers fail.

1. Introduction

Recovery sequences play an important role in the study of the mechanisms underlying the genesis of cardiac arrhythmias, but there are still uncertainties about the best method for determining repolarization times (RTs) from extracellular recordings. Widely used RT markers derived from transmembrane action potentials (TAPs) are the instant RT_{tap} of minimum downslope (fastest repolarization) and the instant $\mathrm{RT90}_{tap}$ when the TAP reaches the 90% of the resting value (late repolarization phase), both during downstroke.

The most widely used RT marker derived from unipolar electrograms (EGs) is the instant RT_{eg} of occurrence of the maximum time derivative during the T wave [1, 2]. We have recently proposed in [3] an EG-based marker for late repolarization, i.e. the instant $\mathrm{RT90}_{eg}$ of minimum second time derivative of the EG waveform during the T wave. The other extracellular technique for determining repolarization times is based on bipolar signals recorded taken the difference between the EG at a fixed site inside an area permanently depolarized (PD), created e.g. by pressure, suction or KCl injection, and the EGs of exploring sites. When the exploring and PD sites are very close to each other, we obtain the so-called monophasic action potential (MAP), see e.g. [4], while when considering a generic exploring site, we obtain the so-called hybrid monophasic action potentials (HMAP), see e.g. [5]. The HMAP is equivalent to a bipolar signal obtained by taking as a reference the potential at a fixed PD site and reversing its polarity. The TAP and MAP techniques can not be performed extensively in in vivo measurements. Conversely, the EG and HMAP extracellular recording techniques can be applied in studying the excitation and repolarization sequences in large regions of a beating heart in in vivo studies. Since the HMAP waveforms exhibit a monophasic downstroke phase, they contain valuable information about the repolarization time of the exploring site, see [6]. Hence, the HMAP-based markers RT_{hmap} and $\mathrm{RT90}_{hmap}$ are defined in the same way as the TAP repolarization markers.

There is a general agreement on the reliability of RTs derived from the MAP signals, since they provide waveforms closed to the TAP signals. On the other hand, the use of the HMAP-based markers is still controversial. To our knowledge, a simulation study on the discrepancies and limitations of the RT_{hmap} and $\mathrm{RT90}_{hmap}$ markers is still missing in the literature, as well as a comparison of

their performance with that of the RT_{eg} and $RT90_{eg}$ markers. The present paper accomplishes this quantitative analysis by means of 3D simulations using the macroscopic Bidomain representation of a portion of the ventricular wall, coupled with the Luo-Rudy phase I system modeling the ionic membrane currents. We simulate the multidimensional propagation of activation and repolarization sequences in an insulated anisotropic cardiac tissue block, also in presence of a subendocardial ischemic region.

2. Methods

The Bidomain model. In the Bidomain model (see [7]), the intra and extracellular potentials $u_i(\mathbf{x},t), u_e(\mathbf{x},t)$, the gating variables $w(\mathbf{x},t)$ and the ionic concentrations $c(\mathbf{x},t)$, are the solutions of the reaction-diffusion system

$$\begin{cases} c_m \dfrac{\partial v}{\partial t} - \mathrm{div}(D_i \nabla u_i) + i_{ion}(v,w,c) = -i_{app} \\ -c_m \dfrac{\partial v}{\partial t} - \mathrm{div}(D_e \nabla u_e) - i_{ion}(v,w,c) = i_{app} \\ \dfrac{\partial w}{\partial t} - R(v,w) = 0, \qquad \dfrac{\partial c}{\partial t} - S(v,w,c) = 0 \\ \mathbf{n}^T D_{i,e} \nabla u_{i,e} = 0 \\ v(\mathbf{x},0) = v_0(\mathbf{x}),\ w(\mathbf{x},0) = w_0(\mathbf{x}),\ c(\mathbf{x},0) = c_0(\mathbf{x}). \end{cases}$$

Here $v(\mathbf{x},t) = u_i(\mathbf{x},t) - u_e(\mathbf{x},t)$ is the transmembrane potential, c_m, i_{ion}, i_{app} the capacitance , the ionic current of the membrane and the applied intra- and extra-cellular currents per unit volume, respectively. The analytic expressions of i_{ion}, R and S depend on the membrane model employed: in our case we use the Luo-Rudy I model (LR1, [8]). The anisotropic conductivity tensors $D_{i,e}$ are built from a fiber structure rotating 90 degrees from endo to epicardium and from a laminar structure yielding an orthotropic anisotropy of the tissue with different conductivity coefficients along the principal axis of the fiber, see [9] for details. The Bidomain system is discretized by finite elements in space and semi-implicit finite differences in time [10]. To ensure parallelization and portability, the code is based on the PETSc parallel library [11]. All simulations are run on a Linux cluster.

Multi-electrode array and electrograms. The cardiac domain H considered in this study is a cartesian slab of dimensions $1.92 \times 1.92 \times 0.48\ cm^3$, modeling a portion of the left ventricular wall. In this slab, we consider a matrix of 12×12 exploring multielectrode needles spaced 1.6 mm from each other and 0.8 mm from the slab boundary, as shown in Fig. 1. Each needle carries 13 recording sites, spaced 0.4 mm along the shank. We then have 12×12 sites on each of the 13 intramural planes, for a total of 12×12×13 = 1872 recording sites in the slab, each recording the intra and extracellular potentials.

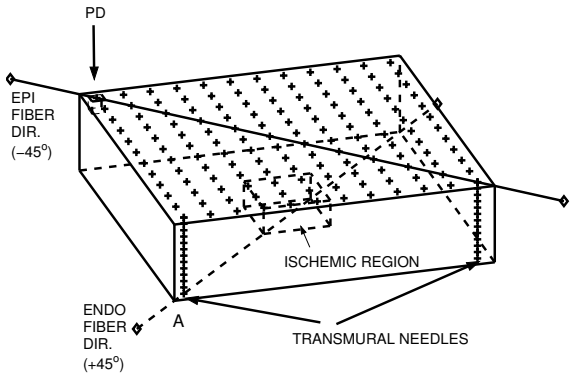

Figure 1. Cardiac slab H, Permanently Depolarized (PD) site, subendocardial ischemic region, transmural needles.

Permanently depolarized (PD) volume. A permanently depolarized (PD) site is obtained by assigning the extracellular potassium concentration equal to the intracellular one, i.e. I_{K1} is zero in the small PD volume. The PD site is labeled PD in Fig. 1 and it has dimensions $0.8 \times 0.8 \times 0.8\ mm^3$. Given a point $\mathbf{x}_{PD}$ in the PD volume, the HMAP at a generic point $\mathbf{x}$ in the domain is given by $hmap(\mathbf{x},t) = u_e(\mathbf{x}_{PD},t) - u_e(\mathbf{x},t)$.

Subendocardial ischemia. We consider three different types of slabs, one with homogeneous intrinsic cellular properties (H-slab), one with a subendocardial moderate ischemic region (MI-slab) and one with an acute ischemic region (AI-slab). The ischemic region has dimensions $0.4 \times 0.4 \times 0.16\ cm^3$ and is located at the center of the slab as shown in Fig. 1. In the LR1 model, the current I_K is scaled by a factor 2.325. Inside the ischemic region, the extracellular potassium concentration $[K]_o$ is increased from $5.4\,mM$ (control) to $10.5\,mM$ (MI-slab) and $18\,mM$ (AI-slab), yielding resting potential and APD90 of $-84\,mV$ and $250\,ms$ (control), $-70\,mV$ and $150\,ms$ (MI-slab), $-55\,mV$ and $60\,ms$ (MI-slab), see [9] for details of the parameters calibration.

Stimulation site. Intra- and extra-cellular stimuli are applied ($i_{app} = -250\ mA/cm^3$ for 1 ms) in a small volume (3 mesh points in each direction) at site A in Fig. 1.

Postprocessing. We saved the extracellular and the intracellular potential waveforms $u_e(x,t)$ and $u_i(x,t)$ at the $12 \times 12 \times 13$ locations of the multi-electrode array. These potential waveforms are defined apart from the same time-dependent constant related to the choice of reference potential. In our simulations, we choose as reference potential the average extracellular potential over the cardiac volume. The waveforms u_e and $v = u_i - u_e$ are then post-processed by computing the repolarization markers defined previously. The TAP markers are assumed to be the gold standard of repolarization time in our reliability analysis of the extracellular RT markers.

	RT_{eg} v RT_{tap}			RT_{hmap} v RT_{tap}		
	mean	std	corr	mean	std	corr
H-slab	2.14	1.98	0.99	1.83	1.60	0.99
MI-slab	2.50	4.26	0.97	2.05	2.99	0.98
AI-slab	2.03	1.80	0.99	1.81	1.53	0.99
global	2.22	2.68	0.98	1.90	2.04	0.99
	$RT90_{eg}$ v $RT90_{tap}$			$RT90_{hmap}$ v $RT90_{tap}$		
	mean	std	corr	mean	std	corr
H-slab	0.97	1.18	0.99	3.04	2.15	0.99
MI-slab	1.30	1.84	0.99	3.07	2.24	0.98
AI-slab	1.12	1.23	0.99	2.95	1.87	0.98
global	1.13	1.42	0.99	3.02	2.09	0.98

Table 1. Recovery times and action potential duration markers discrepancies. mean = average absolute difference between two markers; std = standard deviation of the absolute difference between two markers; corr = correlation coefficient between two markers.

3. Results

We simulate the excitation and repolarization process for the H-slab, MI-slab, AI-slab, elicited by a local stimulus applied at the location A in Fig. 1. We evaluate the global performance of the extracellular markers for the the three simulations, disregarding marker values related to sites within the inexcitable regions, i.e. the PD volume and the ischemic region in the AI case.

Table 1 reports the comparison between the RT markers (RT_{eg} vs RT_{tap}, RT_{hmap} vs RT_{tap}, $RT90_{eg}$ vs $RT90_{tap}$, $RT90_{hmap}$ vs $RT90_{tap}$). The results show that all the extracellular repolarization markers provide very reliable estimates of the reference transmembrane markers, with correlation coefficients always greater than 0.97. This good match between the extracellular repolarization markers and the reference TAP-based markers is also confirmed by Fig. 2, reporting the regression plots of RT_{eg} vs RT_{tap} and RT_{hmap} vs RT_{tap} for all three simulations. In terms of accuracy, the $RT90_{eg}$ marker exhibits the best performance, with discrepancies $RT90_{eg}$ - $RT90_{tap}$ ranging between -5 and $5\,ms$. The RT_{eg} and RT_{hmap}, as estimates of RT_{tap}, show comparable global performance, because both the averages of $|RT_{eg} - RT_{tap}|$ and $|RT_{hmap} - RT_{tap}|$ are about $2\,ms$. Despite a global correlation coefficient of 0.98, the $RT90_{hmap}$ marker exhibits the largest discrepancies, ranging between -10 and $10\,ms$.

The repolarization maps constructed from RT_{eg} and RT_{hmap} confirm that these extracellular markers are able to reproduce the main qualitative features of the repolarization sequences in the homogeneous slab and also in presence of the subendocardial ischemic region. This is confirmed by the repolarization maps displayed in Fig. 3 for MI-slab, where the largest discrepancies arise in the transmural region above the ischemic area.

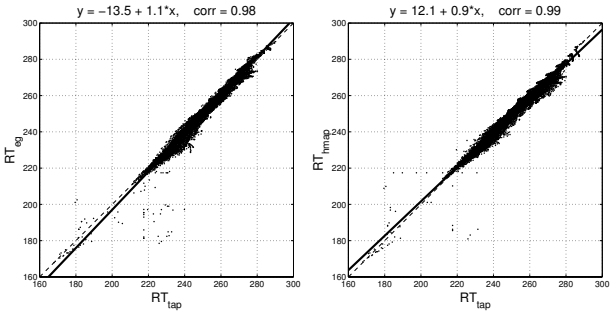

Figure 2. Regression lines of RT_{eg} vs RT_{tap} (first row), RT_{hmap} vs RT_{tap} (second row).

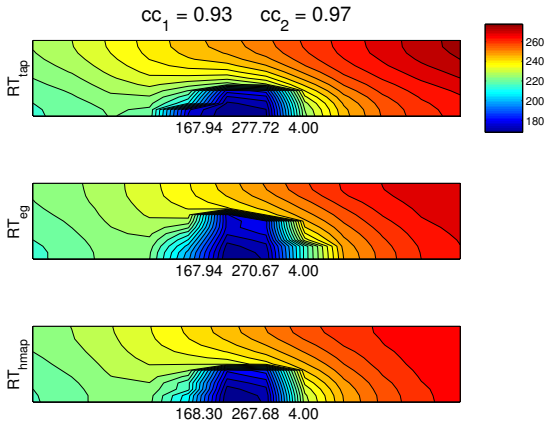

Figure 3. MI-slab. Recovery maps on a transmural diagonal section issuing from A of Fig. 1 from multi-electrode array markers RT_{tap} (top panel), RT_{eg} (middle panel) and RT_{hmap} (bottom panel).

Figs. 4-top (MI-slab) and -bottom (AI-slab) show the TAP, EG and HMAP waveforms at some sample points located in the transmural region above the ischemic area, where the extracellular markers may be inaccurate. A first critical morphology of the EG waveform, often found in experimental setup, consists in an almost linear increasing variation during the ST segment. Generally, when the RT_{eg} is applied to these EG signals, it provides a very inaccurate estimate of RT_{tap}. A second critical EG morphology arises near the ischemic inexcitable region (AI-slab), where the waveform does not exhibit a T wave, but often a weakly monophasic component, thus the RT_{eg} marker fails. In both cases, the HMAP waveforms exhibit a monophasic downstroke component, from which a well defined RT_{hmap} is derived providing a reliable alternative estimate of RT_{tap}. Instead, in these cases, both $RT90_{eg}$ and $RT90_{hmap}$ are reliable estimates of $RT90_{tap}$, with $RT90_{hmap}$ being more accurate than $RT90_{eg}$.

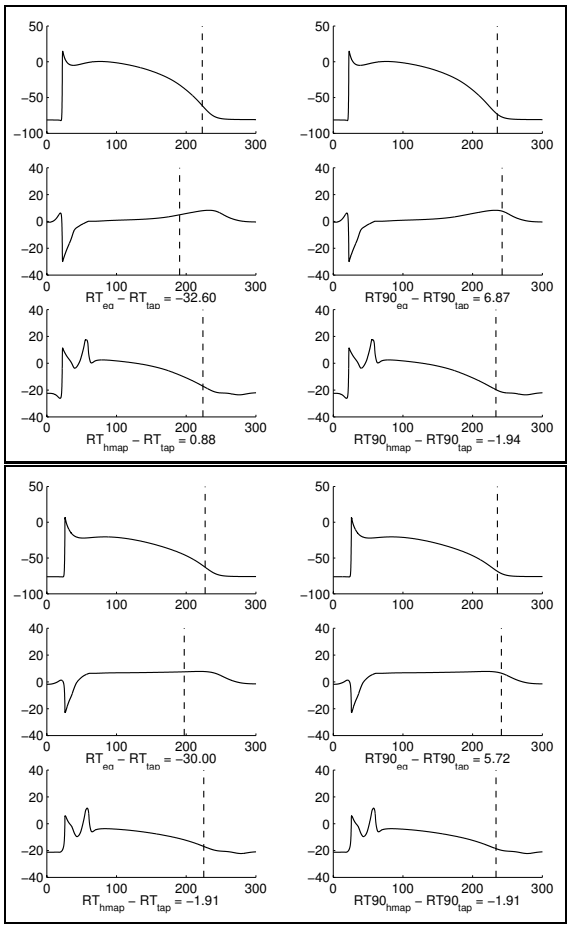

Figure 4. Top panel: MI-slab, TAP (first row), EG (second row) and HMAP (third row) waveforms in a midmyocardial site. The vertical lines in the left columns indicate RT_{tap} (first row), RT_{eg} (second row) and RT_{hmap} (third row), those in the right columns indicate $\mathrm{RT90}_{tap}$ (first row), $\mathrm{RT90}_{eg}$ (second row) and $\mathrm{RT90}_{hmap}$ (third row). Bottom panel: AI-slab, same format as the top panel.

4. Conclusion

The results of the quantitative analysis presented, based on 3D Bidomain numerical simulations, show a very high average correlation coefficient (0.98) between the EG- and HMAP-based markers RT_{eg}, RT_{hmap}, $\mathrm{RT90}_{eg}$,$\mathrm{RT90}_{hmap}$ and the reference TAP-based markers RT_{tap} and $\mathrm{RT90}_{tap}$, respectively. Regarding the RT_{eg} marker, our findings agree with the recent works [3,12]. This good global match assures a high reliability of the markers in terms of localizing the regions that repolarize first and last and in terms of the intramural and transmural repolarization pathways. Nevertheless, at recording sites located inside or near the borders of the ischemic region, RT_{eg} may fail as estimate of RT_{tap}, because e.g. of linear ramp of the T wave or absence of T wave, as already observed in [13]. In these critical cases, RT_{hmap} is a reliable alternative for estimating RT_{tap}.

References

[1] Wyatt R. Comparison of estimates of activation and recovery times from bipolar and unipolar electrograms to in vivo transmembrane action potential durations. In Proc. IEEE/Eng. Med. Biol. Soc. 1980; 22–25.

[2] Haws C, Lux R. Correlation between in vivo transmembrane action potential durations and activation– recovery intervals from electrograms. Circulation 1990;81:281–288.

[3] Colli Franzone P, Pavarino L, Scacchi S, Taccardi B. Determining recovery times from transmembrane action potentials and unipolar electrograms in normal heart tissue. In Sachse F, Seemann G (eds.), FIMH07, volume 4466 of LNCS. Springer, 2007; 139–149.

[4] Franz M. Monophasic Action Potentials: Bridging Cells to Bedside. Futura Publishing Company, 2000.

[5] Nesterenko V, Weissenburger J, Antzelevitch C. Hybrid action potential etiology. cellular basis and method for recording the monophasic action potential. J Cardiovasc Eletrophysiol 2000;11:948–951.

[6] Colli Franzone P, Pavarino L, Scacchi S, B T. Monophasic action potentials generated by bidomain modeling as a tool for detecting cardiac repolarization times. Am J Physiol Heart Circ Physiol 2007;293:H2771–H2785.

[7] Henriquez C. Simulating the electrical behavior of cardiac tissue using the bidomain model. Crit Rev Biomed Eng 1993;21:1–77.

[8] Luo C, Rudy Y. A model of the ventricular cardiac action potential: depolarization, repolarization, and their interaction. Circ Res 1991;68(6):1501–1526.

[9] Colli Franzone P, Pavarino L, Scacchi S. Dynamical effects of myocardial ischemia in anisotropic cardiac models in three dimensions. Math Mod Meth Appl Sci 2007; 17(12):1965–2008.

[10] Colli Franzone P, Pavarino L. A parallel solver for reaction-diffusion systems in computational electrocardiology. Math Mod Meth Appl Sci 2004;14(6):883–911.

[11] Balay S, Buschelman K, Gropp D, Kaushik D, Knepley M, Curfman McInnes L, Smith B, Zhang H. PETSc Web page, 2001. Http://www.mcs.anl.gov/petsc.

[12] Potse M, Coronel R, Opthof T, Vinet A. The positive t wave. Anadolu Kardiyol Derg 2007;7(1):164–167.

[13] Steinhaus B. Estimating cardiac transmembrane activation and recovery times from unipolar and bipolar extracellular electrograms: a simulation study. Circ Res 1989; 64(3):449–462.

Address for correspondence:

Simone Scacchi

Dept. of Mathematics/ Università di Pavia

Via Ferrata 1/ 27100 Pavia / Italy

simone.scacchi@unipv.it